Proline Coordination with Fatty Acid Synthesis and Redox Metabolism of Chloroplast and Mitochondria[1][OPEN]

Suhas Shinde[2], Joji Grace Villamor[3], Wendar Lin, Sandeep Sharma[4], and Paul E. Verslues*

Institute of Plant and Microbial Biology, Academia Sinica, Taipei 115, Taiwan

ORCID ID: 0000-0002-7462-5113 (Sa.S.).

Proline (Pro) accumulation is one of the most prominent changes in plant metabolism during drought and low water potential; however, the regulation and function of Pro metabolism remain unclear. We used a combination of forward genetic screening based on a *Proline Dehydrogenase1* (*PDH1*) promoter-luciferase reporter ($PDH1_{pro}$:*LUC2*) and RNA sequencing of the Pro synthesis mutant *p5cs1-4* to identify multiple loci affecting Pro accumulation in Arabidopsis (*Arabidopsis thaliana*). Two mutants having high $PDH1_{pro}$:*LUC2* expression and increased Pro accumulation at low water potential were found to be alleles of *Cytochrome P450, Family 86, Subfamily A, Polypeptide2* (*CYP86A2*) and *Long Chain Acyl Synthetase2* (*LACS2*), which catalyze two successive steps in very-long-chain fatty acid (VLCFA) synthesis. Reverse genetic experiments found additional VLCFA and lipid metabolism-related mutants with increased Pro accumulation. Altered cellular redox status is a key factor in the coordination of Pro and VLCFA metabolism. The NADPH oxidase inhibitor diphenyleneiodonium (DPI) induced high levels of Pro accumulation and strongly repressed $PDH1_{pro}$:*LUC2* expression. *cyp86a2* and *lacs2* mutants were hypersensitive to diphenyleneiodonium but could be reverted to wild-type Pro and $PDH1_{pro}$:*LUC2* expression by reactive oxygen species scavengers. The coordination of Pro and redox metabolism also was indicated by the altered expression of chloroplast and mitochondria electron transport genes in *p5cs1-4*. These results show that Pro metabolism is both influenced by and influences cellular redox status via previously unknown coordination with several metabolic pathways. In particular, Pro and VLCFA synthesis share dual roles to help buffer cellular redox status while producing products useful for stress resistance, namely the compatible solute Pro and cuticle lipids.

Pro accumulation occurs in many plant species and can be induced by several types of abiotic stresses, including drought (Szabados and Savouré, 2010; Verslues and Sharma, 2010). Altered Pro metabolism also can have effects on plant development (Funck et al., 2012; Mattioli et al., 2012; Kavi Kishor et al., 2015). Of the many stimuli that can influence Pro, it is drought and low water potential (ψ_w) that induce the highest levels of Pro accumulation. There has been considerable effort to modify Pro metabolism to enhance drought resistance (Zhu et al., 1998; Nanjo et al., 1999; Roosens et al., 2002; Sawahel and Hassan, 2002; de Ronde et al., 2004; Su and Wu, 2004; Gleeson et al., 2005). Such efforts have been impeded by unresolved questions regarding why plants accumulate Pro and how it contributes to drought tolerance. Substantial evidence indicates a role for Pro in osmotic adjustment based on both the high levels of Pro accumulation and observations that it accumulates predominantly in the relatively small volume of the cytoplasm and organelles (Voetberg and Sharp, 1991; Bussis and Heineke, 1998). However, osmotic adjustment is not the only role of Pro accumulation. More recent data have emphasized the connection of Pro to redox status (Sharma et al., 2011; Ben Rejeb et al., 2014, 2015) and demonstrated that both Pro synthesis and catabolism are essential to promote drought tolerance (Sharma et al., 2011; Bhaskara et al., 2015). The overall picture that emerges is that both the level of Pro accumulated as well as the turnover of Pro and its connection to broader metabolic status must be considered to fully understand the role of Pro metabolism in drought resistance (Szabados and Savouré, 2010; Bhaskara et al., 2015).

[1] This work was supported the Taiwan Ministry of Science and Technology (grant no. NSC 102–2628–B–001–003 to P.E.V.) and by an Academia Sinica Career Development Award to P.E.V.

[2] Present address: Department of Biological Sciences, East Tennessee State University, Johnson City, TN 37614.

[3] Present address: Protease Degradomics Group, Central Institute for Engineering, Electronics, and Analytics, Forschungszentrum Jülich, 52425 Juelich, Germany.

[4] Present address: Marine Biotechnology and Ecology Division, Central Salt and Marine Chemicals Research Institute, Bhavnagar, Gujarat, 364001 India.

* Address correspondence to paulv@gate.sinica.edu.tw.

The author responsible for distribution of materials integral to the findings presented in this article in accordance with the policy described in the Instructions for Authors (www.plantphysiol.org) is: Paul E. Verslues (paulv@gate.sinica.edu.tw).

Su.S. analyzed mutants and transgenic plants, analyzed data, assisted in article writing, and performed all other experiments not attributed to other authors; J.G.V. constructed the promoter-reporter line and did preliminary experiments for the mutant screen; W.L. analyzed mRNA sequencing data and single-nucleotide polymorphism data for mapping; Sa.S. prepared samples for RNA sequencing and analyzed data; P.E.V. conceived and planned research, analyzed data, and prepared the article with assistance from Su.S.

[OPEN] Articles can be viewed without a subscription.

www.plantphysiol.org/cgi/doi/10.1104/pp.16.01097

Pro is synthesized by the conversion of Glu to the intermediate Δ^1-pyrroline-5-carboxylate (P5C) by P5C synthetase (P5CS), and P5C is then converted to Pro by P5C reductase (P5CR; Szabados and Savouré, 2010; Verslues and Sharma, 2010). P5CS utilizes NADPH as a cofactor (Zhang et al., 1995). P5CR can utilize both NADH and NADPH; however, recent work indicates that NADPH is the predominant source of reductant used by P5CR in vivo (Giberti et al., 2014). Arabidopsis (*Arabidopsis thaliana*) has two *P5CS* genes that are not functionally equivalent (Székely et al., 2008). *P5CS1* is induced by drought and related stresses at both the transcript and protein levels and is thought to be the rate-limiting step for stress-induced Pro synthesis. *p5cs1* mutants have greatly reduced Pro accumulation during low ψ_w or salt stress but have normal growth and morphology under unstressed conditions (Székely et al., 2008; Sharma et al., 2011; Bhaskara et al., 2015). Despite many stress-related studies that have measured or manipulated *P5CS1* gene expression, how P5CS1-mediated Pro synthesis is regulated and interacts with other metabolic pathways is still unclear.

Pro catabolism occurs in the mitochondria via proline dehydrogenase (PDH), which converts Pro to P5C, and P5C dehydrogenase (P5CDH), which converts P5C back to Glu, thus forming the Pro cycle (Szabados and Savouré, 2010; Verslues and Sharma, 2010). A unique feature of PDH is that it donates electrons directly to the mitochondrial electron transport chain; however, mechanistic details and the identity of the electron acceptor are not firmly established in plants (Szabados and Savouré, 2010; Verslues and Sharma, 2010). Of the two Arabidopsis genes that encode PDH, *PDH1* is more highly expressed and is thought to have a predominant role in Pro catabolism (Funck et al., 2010). *PDH1* expression is down-regulated by drought stress in much of the plant (Peng et al., 1996; Yoshiba et al., 1997; Sharma and Verslues, 2010). Conversely, *PDH1* is induced by exogenous Pro, and this induction involves a cis-element containing the sequence ACTCAT, referred to as the proline response element (ProRE; Satoh et al., 2002). The ProRE is bound by several bZIP transcription factors that can up-regulate *PDH1* in response to exogenous Pro, starvation, and perhaps other signals (Satoh et al., 2004; Weltmeier et al., 2006; Dietrich et al., 2011). The upstream factors that regulate the activity of these bZIPs are not known. The up-regulation of *PDH1* in response to Pro presents an unresolved paradox. During drought stress, a high level of Pro accumulates; yet, rather than be induced by this high level of Pro, *PDH1* is down-regulated in most plant tissues (Miller et al., 2005). Thus, *PDH1* is regulated by incompletely understood mechanisms that likely reflect both stress and metabolic signals. All these factors make *PDH1* an excellent marker to study the intersection of stress signaling and metabolic regulation.

We used a forward genetic screen based on the expression of a *PDH1 promoter:Luciferase* construct combined with mapping by sequencing to identify factors affecting *PDH1* expression and Pro accumulation. This screen found an unexpected effect of very-long-chain fatty acid (VLCFA) synthesis on Pro accumulation. Several lines of evidence indicate that reduced VLCFA synthesis affects Pro accumulation via effects on redox status rather than signaling functions of VLCFA metabolism enzymes or lipid metabolism intermediates. In parallel, mRNA sequencing of *p5cs1-4*, which has reduced Pro synthesis, found substantial effects on chloroplast and mitochondria gene expression consistent with a connection of Pro to redox metabolism in both organelles. Together, these results show the extensive coordination of Pro metabolism with multiple metabolic pathways related to cellular redox status.

RESULTS

A Mutant Screen Based on the *PDH1* Promoter Identifies Mutants of *Cytochrome P450, Family 86, Subfamily A, Polypeptide2* and *Long Chain Acyl Synthetase2* with Increased Pro Accumulation at Low ψ_w

A forward genetic screen was developed to identify factors affecting *PDH1* expression and Pro accumulation. A 1.5-kb fragment of the *PDH1* promoter and 5′ untranslated region (UTR) was used to drive the expression of the Luciferase2 reporter ($PDH1_{pro}$:*LUC2*). Several Arabidopsis (Columbia-0 [Col-0] accession) transgenic lines containing single-locus insertions of the $PDH1_{pro}$:*LUC2* reporter were isolated. A single line having 5-fold down-regulation of $PDH1_{pro}$:*LUC2* in response to low ψ_w, essentially identical to the endogenous *PDH1* (Fig. 1; Sharma and Verslues, 2010), was selected for further study. This unmutagenized $PDH1_{pro}$:*LUC2* line is referred to as wild type (W.T.) in

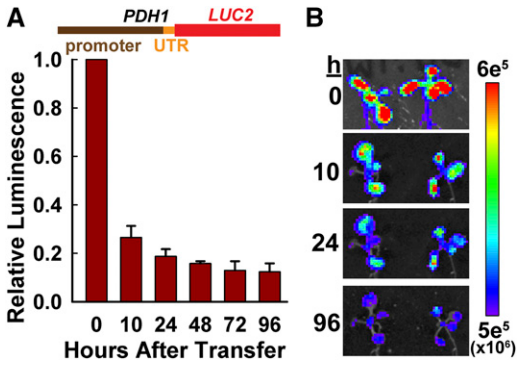

Figure 1. A $PDH1_{pro}$:*LUC2* reporter responsive to low ψ_w. A, The *PDH1* promoter and 5′ UTR were fused to the *LUC2* coding region and used to generate transgenic plants. Quantitation of $PDH1_{pro}$:*LUC2* luminescence in shoot tissue of seedlings transferred to low ψ_w (−1 MPa) for the indicated lengths of time is shown. Data are means ± SE (n = 6). B, Representative false-color images of luminescence intensity from the experiments reported in A. The intensity scale for the images is shown at right.

subsequent figures. After ethyl methanesulfonate (EMS) mutagenesis, screening in the M1 and M2 generations (Supplemental Fig. S1) identified mutants with high or low $PDH1_{pro}$:*LUC2* expression. Candidate genes for a number of high-$PDH1_{pro}$:*LUC2* mutants were identified using a mapping-by-sequencing approach, and two such mutants are reported here.

Mutants 4442-4 and 4255-1 were phenotypically similar, with each one having 3-fold increased $PDH1_{pro}$:*LUC2* expression in both control and stress treatments (Fig. 2, A and B). Low ψ_w could still repress the expression of $PDH1_{pro}$:*LUC2* in 4442-4 and 4255-1, but not to the level seen in the wild type. Also, both mutants had Pro accumulation nearly twice that of the wild type at −1.2 MPa (Fig. 2C) but did not differ from the wild type in the Pro content of unstressed plants. Expression of the endogenous *PDH1* was increased approximately 3-fold in 4442-4 under unstressed conditions (Fig. 2D) and agreed well with the increased $PDH1_{pro}$:*LUC2* expression. However, at low ψ_w, *PDH1* expression decreased to a level similar to that in the wild type, despite the higher $PDH1_{pro}$:*LUC2* expression (Fig. 2D). A similar difference between $PDH1_{pro}$:*LUC2* expression and endogenous *PDH1* at low ψ_w also was observed in other high-Pro, high-$PDH1_{pro}$:*LUC2* mutants in our collection (S. Mukuri, S. Shinde, and P.E. Verslues, unpublished data).

For 4442-4, sequencing of bulked segregants and next-generation mapping (Austin et al., 2011) identified several candidate genes (Supplemental Fig. S2A). However, only mutants of *Cytochrome P450, Family 86, Subfamily A, Polypeptide 2* (*cyp86a2*; At4g00360) had elevated Pro levels similar to 4442-4 (Fig. 3A). Mutants of the two other candidate genes did not differ from the wild type in Pro accumulation (Supplemental Fig. S2B). For 4255-1, *Long Chain Acyl Synthetase2* (*LACS2-1*; At1g49430) was identified as the main candidate gene (Supplemental Fig. S2C), and *lacs2-1* (Schnurr et al., 2004) had increased Pro accumulation similar to 4255-1 (Fig. 3A). Genetic complementation found that F1 seedlings of 4442-4 crossed to *cyp86a2-1* as well as 4255-1 crossed to *lacs2-1* had the same high $PDH1_{pro}$:*LUC2* expression as the homozygous mutant (Fig. 3B). This indicated that 4442-4 was an allele of *cyp86a2* and 4255-1 was an allele of *lacs2*.

Both LACS2 and CYP86A2 are endoplasmic reticulum-localized enzymes that catalyze successive steps in VLCFA synthesis: the esterification of C_{16} and C_{18} fatty acids to CoA and subsequent ω-hydroxylation of these

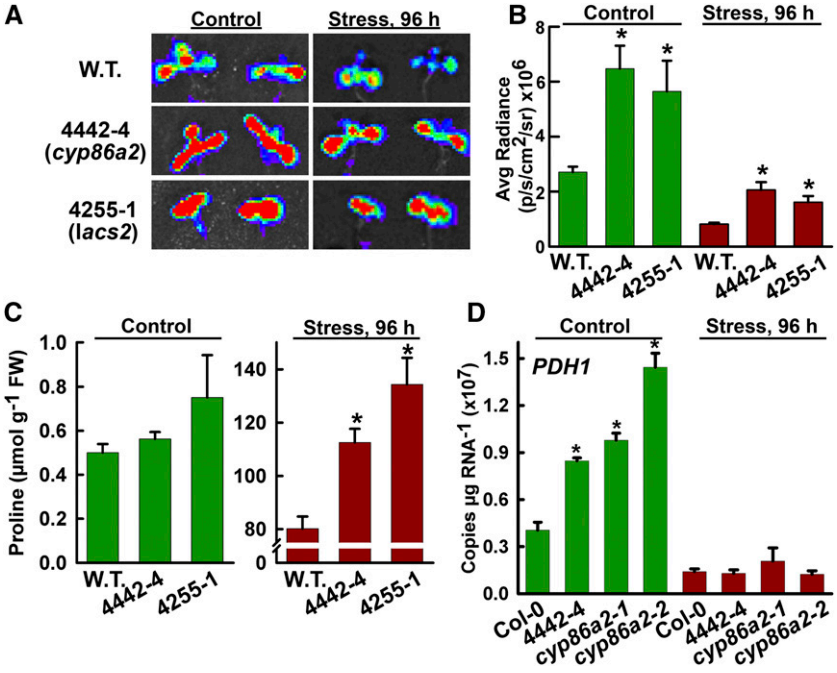

Figure 2. Mutants 4442-4 and 4255-1 have increased $PDH1_{pro}$:*LUC2* activity and increased Pro accumulation at low ψ_w. A, Representative false-color luminescence images of the wild type (W.T.) and mutants in the unstressed control and after 96 h at −1 MPa low-ψ_w treatment. B, Quantification of $PDH1_{pro}$:*LUC2* activity in 4442-4 and 4255-1. Data are means ± SE (n = 4–15). Significant differences ($P \geq 0.05$) compared with the wild type in the same treatment are marked with asterisks. Luminescence intensities are given in photons (p) per second (s) per cm^2 per steradian (sr). C, Pro accumulation in unstressed control (−0.25 MPa) or low-ψ_w stress (−1.2 MPa) for the wild type and mutants. FW, Fresh weight. Data are means ± SE (n = 3–9). Significant differences ($P \geq 0.05$) compared with the wild type in the same treatment are marked with asterisks. Note that the wild type is the unmutagenized $PDH1_{pro}$:*LUC2* line for all experiments in A to C. D, *PDH1* gene expression in Col-0 wild type, 4442-4, and two T-DNA alleles of *cyp86a2* in the unstressed control treatment or at 96 h after transfer to −1.2-MPa stress. Data are means ± SE (n = 3). Significant differences ($P \geq 0.05$) compared with the wild type in the same treatment are marked with asterisks. The expression of additional Pro metabolism genes in these mutants is shown in Supplemental Figure S4.

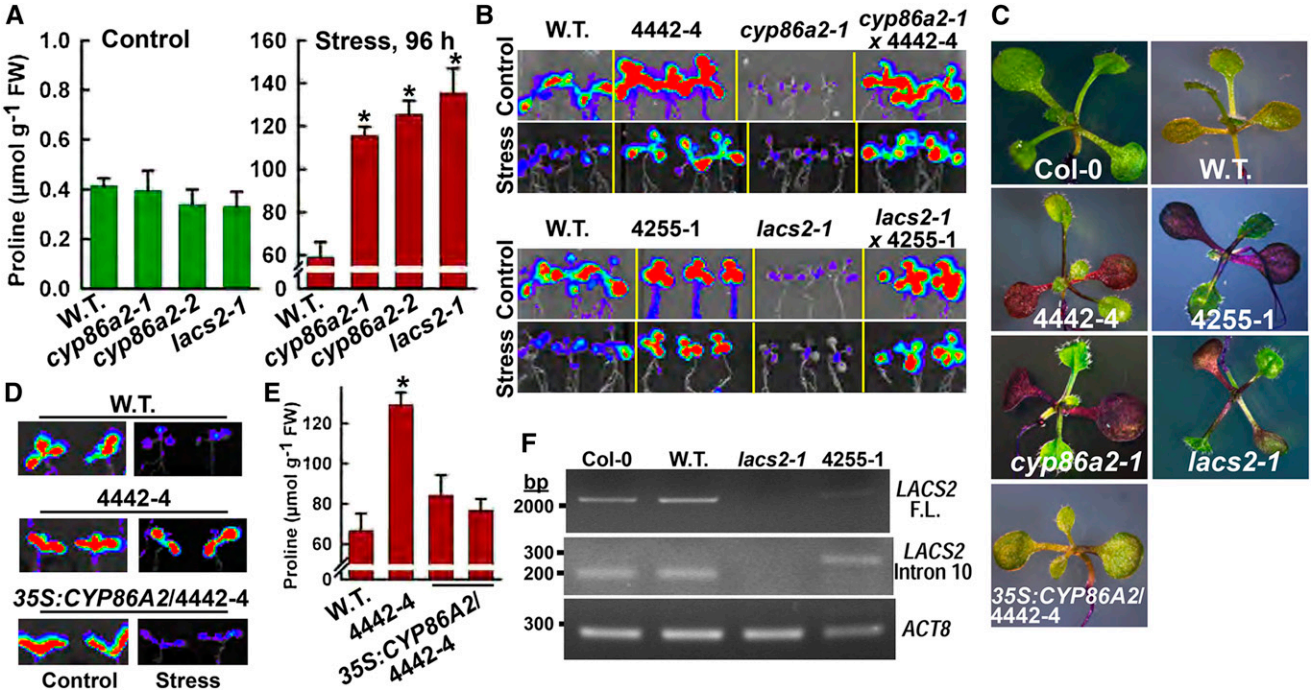

Figure 3. 4442-4 and 4255-1 are alleles of *cyp86a2* and *lacs2*, respectively. A, Pro accumulation in two *cyp86a2* T-DNA alleles and *lacs2-1* under control and −1.2-MPa low ψ_w stress treatments. FW, Fresh weight. Data are means ± SE (n = 4–6) from two experiments. Significant differences ($P \geq 0.05$) compared with the wild type (W.T.) in the same treatment are marked with asterisks. B, $PDH1_{pro}$:*LUC2* imaging in F1 seedlings of crosses of 4442-4 and 4255-1 with *cyp86a2-1* and *lacs2-1*, respectively, along with wild-type $PDH1_{pro}$:*LUC2* and mutant seedlings as controls. C, Toluidine Blue staining using seedlings of Col-0, wild-type $PDH1_{pro}$:*LUC2*, as well as mutants and a transgenic complemented line of 4442-4. D, $PDH1_{pro}$:*LUC2* imaging of wild-type $PDH1_{pro}$:*LUC2*, 4442-4, and 4442-4 complemented with *35S:CYP86A2*. Stress treatment was −1 MPa for 96 h. E, Stress-induced (−1.2 MPa, 96 h) Pro accumulation in 4442-4 and two independent T3 lines of 4442-4 complemented with *35S:CYP86A2*. Data are means ± SE (n = 4–6) from two experiments. Significant differences ($P \geq 0.05$) compared with the wild type in the same treatment are marked with asterisks. F, Reverse transcription (RT)-PCR analysis of Col-0, wild-type $PDH1_{pro}$:*LUC2*, *lacs2-1*, and 4255-1 using primers to amplify the full-length LACS2 RNA or the region around intron 10. *ACTIN8* (*ACT8*) was used as a reference gene.

fatty acids for the synthesis of cutin monomers (Li-Beisson et al., 2013). EMS mutants 4442-4 and 4255-1 stained with Toluidine Blue (Fig. 3C), indicating that they share the previously reported cuticle defects of *cyp86a2* and *lacs2* (Schnurr et al., 2004; Xiao et al., 2004). We also transgenically complemented 4442-4 with *35S:CYP86A2* (Fig. 3, C–E) and showed that introducing the *cyp86a2-1* and *lacs2-1* T-DNA mutants into the $PDH1_{pro}$:*LUC2* background produced the same high $PDH1_{pro}$:*LUC2* expression phenotype as the 4442-4 and 4255-1 EMS mutants (Supplemental Fig. S3). 4442-4 has a point mutation that changes Gly-37 to Asp (G-to-A transition at position 110 of the *CYP86A2* coding sequence). This mutation lies in the catalytic domain (amino acids 5–511 based on the National Center for Biotechnology Information's conserved domain database search), consistent with 4442-4 being a null allele of CYP86A2. For 4255-1, the mutation was in a cryptic splice site at the *LACS2* intron 10-exon 11 junction (G-to-A transition at position 18,293,272 of chromosome 1). Primers spanning intron 10 amplified a larger fragment in 4255-1 than in the wild type (Fig. 3F), consistent with retention of the 84-bp intron 10. This alters the downstream reading frame, thus preventing the translation of functional LACS2 protein.

Further characterization of 4442-4 and 4255-1 as well as *cyp86a2-1* and *lacs2-1* T-DNA mutants found that the protein abundance and apparent M_r of PDH1 and P5CS1 were not altered in any of the mutants under either stress or control conditions (Fig. 4A). Thus, *cyp86a2* and *lacs2* did not affect the posttranslational regulation (e.g. redox-related posttranslational modifications; see below) of these two key enzymes of Pro metabolism. *P5CS1* gene expression, as well as the expression of other Pro metabolism genes, also was not substantially altered in *cyp86a2* mutants (Supplemental Fig. S4). Further experiments with *cyp86a2* mutants found that they had increased Pro across a range of low ψ_w severities, with even a mild stress of −0.5 MPa leading to twice as much Pro accumulation in *cyp86a2* as in the wild type (Fig. 4B). Interestingly, *cyp86a2* had the same Pro accumulation as the wild type in response to salt stress or exogenous abscisic acid (Fig. 4B). Thus, the effect of disrupting VLCFA synthesis on Pro was specific to low ψ_w and occurred via an unknown mechanism that did not involve altered gene expression or modification of the two key Pro metabolism enzymes P5CS1 and PDH1.

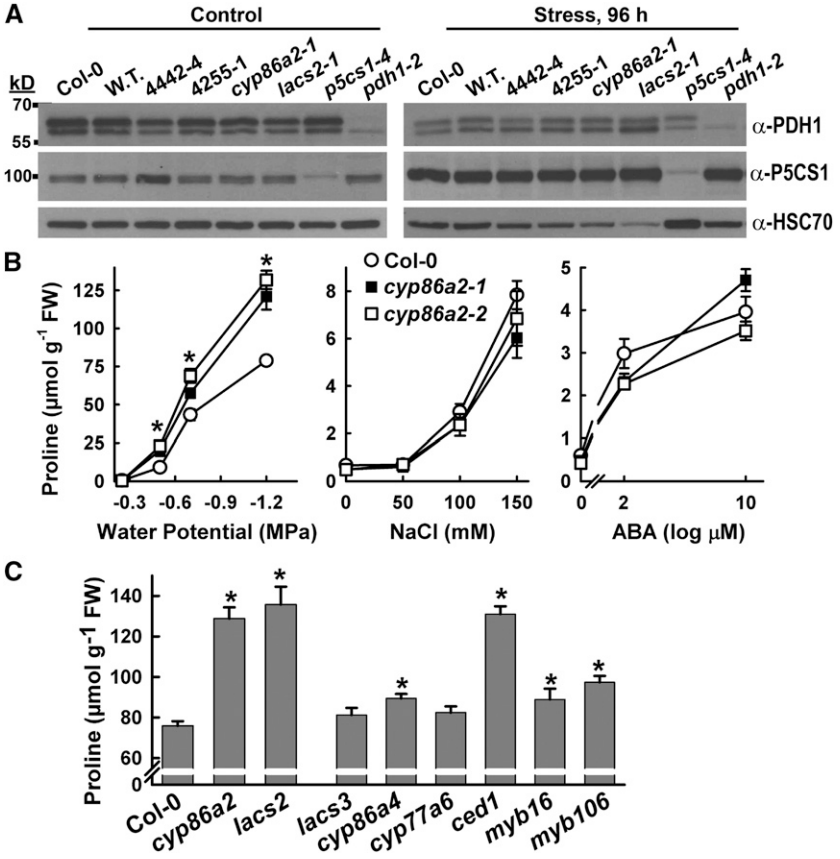

Figure 4. Effects of *cyp86a2* and *lacs2* mutants on Pro metabolism and the identification of additional cuticle lipid-related mutants with increased Pro accumulation at low ψ_w. A, Western blots of PDH1 and P5CS1 protein levels in Col-0, wild-type $PDH1_{pro}$:*LUC2* (W.T.), and *cyp86a2* and *lacs2* mutants. *p5cs1-4* and *pdh1-2* were included to show the specificity of the antisera. Blots were stripped and reprobed with antisera recognizing HSC70 as a loading control. A total of 50 μg of protein was loaded in each lane. B, Effects of a range of low-ψ_w, salt, or abscisic acid (ABA) treatments on Pro accumulation of the Col-0 wild type and *cyp86a2* mutants. FW, Fresh weight. Data are means ± SE (n = 8–12) from two experiments. Significant differences ($P \geq 0.05$) compared with the wild type in the same treatment are marked with asterisks. C, Stress-induced (−1.2 MPa, 96 h) Pro accumulation in cuticle metabolism mutants. Data are means ± SE (n = 11–24) from two experiments. Significant differences ($P \geq 0.05$) compared with the wild type are marked with asterisks. For *ced1*, *cyp77a6*, and *cyp86a4*, the data shown are combined from two to three T-DNA alleles that had identical phenotypes. Additional information and RT-PCR verification of T-DNA mutants can be found in Supplemental Figure S10.

Additional Mutants Affecting VLCFA Synthesis or Cuticle Deposition Also Have Increased Pro Accumulation

The fact that both *CYP86A2* and *LACS2* were identified in our mutant screen suggested that the high Pro accumulation and increased $PDH1_{pro}$:*LUC2* expression may not be due to a specific signaling or enzymatic function of the CYP86A2 and LACS2 proteins. As VLCFAs have been shown to have a signaling function in controlling development (Nobusawa et al., 2013), there were several possible ways in which VLCFA metabolism could influence Pro accumulation and $PDH1_{pro}$:*LUC2* expression. We hypothesized that reduced flux through VLCFA synthesis, reduced levels of a product downstream of CYP86A2, or increased levels of a lipid species upstream of LACS2 could cause the Pro-related phenotypes of *cyp86a2* and *lacs2* mutants. As one way to test these possibilities, we isolated T-DNA mutants of other genes involved in VLCFA metabolism or its regulation. Of these, a mutant of *BODYGUARD/9-CIS EPOXYCAROTENOID DEFECTIVE1* (*CED1*), a cuticle lipid transporter found previously to affect the abiotic stress response (Wang et al., 2011b), had increased Pro accumulation similar to *cyp86a2* and *lacs2-1* (Fig. 4C). Because CED1 functions downstream of *cyp86a2* and *lacs2*, these data indicated that it was not a reduced level of a lipid intermediate downstream of CYP86A2 that increased Pro accumulation. Rather, the blockage of VLCFA metabolism itself seemed a more likely cause. Consistent with this hypothesis, mutants of other VLCFA-related genes had moderate, but significant, increases in Pro accumulation (Fig. 4C), likely reflecting the extent that VLCFA synthesis was disrupted. *CYP86A4* and *CYP77A6* are most active in flowers, with a lesser effect on leaf cuticle (Li-Beisson et al., 2009), and had moderately increased or unaffected Pro accumulation (Fig. 4C). Similarly, MYB16 and MYB106 have overlapping functions, such that each single mutant causes only a partial blockage of flux through VLCFA synthesis (Oshima et al., 2013), and, thus, only a moderate effect on Pro accumulation. Other mutants or inhibitor treatments affecting lipid metabolism upstream of LACS2 also had high Pro levels (see below), further indicating that reduced metabolic flux through lipid metabolism was the most likely cause of increased Pro accumulation in *cyp86a2* and *lacs2-1*.

Cellular Redox Status Is a Factor in Coordinating Pro and VLCFA Metabolism

Pro and VLCFA synthesis lead to different products and occur in different cellular compartments. However, a commonality is that both Pro and VLCFA synthesis consume NADPH and regenerate $NADP^+$ (Sharma et al., 2011; Li-Beisson et al., 2013; Giberti et al., 2014; Ben Rejeb et al., 2015) and, thus, can influence cellular

redox status. To determine whether altered redox status was involved in the high-Pro and high-*PDH1*$_{pro}$:*LUC2* expression of *cyp86a2* and *lacs2*, dithiothreitol (DTT) was used to increase reductant load, while the reactive oxygen species (ROS) scavengers ascorbic acid (AsA) and *N*,*N*′-dimethylthiourea (DMTU) or the NADPH oxidase inhibitor diphenyleneiodonium (DPI) were used to decrease reductant load and interfere with ROS signaling.

Treatment of unstressed Col-0 (wild type) with 5 or 20 mM DTT increased Pro accumulation 4- or 30-fold, respectively (Fig. 5A). This was in agreement with previous results (Kolbe et al., 2006). *cyp86a2-1* and *lacs2-1* had greater response of Pro accumulation to DTT (Fig. 5A). This was consistent with these mutants having altered redox status or less capacity to buffer redox status. Pro accumulation of *pdh1-2* also was more responsive to DTT, while *p5cs1-4* was less responsive, indicating that both Pro synthesis and Pro catabolism were involved in the response to DTT (Fig. 5A). We also observed that 20 mM, but not 5 mM, DTT increased Pro accumulation at low ψ_w (Fig. 5B). Note that we did not analyze Pro in mutants treated with 20 mM DTT or mutants treated with a combination of DTT and low ψ_w, because the mutants were more sensitive to these treatments and exhibited bleaching and seedling death. Conversely, the ROS scavengers AsA and DMTU suppressed low-ψ_w-induced Pro accumulation of *cyp86a2-1* and *lacs2-1* back to the wild-type level (Fig. 5C). AsA and DMTU also significantly inhibited the increased *PDH1*$_{pro}$:*LUC2* expression of 4442-4 and 4255-1 at low ψ_w (Fig. 5, D and F). DMTU also blocked the increased *PDH1*$_{pro}$:*LUC2* expression of unstressed 4442-4 and 4255-1 (Fig. 5E).

Also consistent with a role of redox or ROS in Pro regulation, blocking NADPH oxidase activity using the inhibitor DPI caused a nearly 30-fold increase in Pro content of Col-0 seedlings at high ψ_w (Fig. 6A). DPI treatment of unstressed wild-type seedlings (−0.25 MPa) completely suppressed *PDH1*$_{pro}$:*LUC2* expression to the level typically seen at low ψ_w (Fig. 6B). An even greater response to DPI was seen in *cyp86a2-1*, *lacs2-1*, and *pdh1-2*, as Pro content increased 50- to 60-fold over the untreated control and *PDH1*$_{pro}$:*LUC2* activity was suppressed to the wild-type level (Fig. 6, A and B; −0.25 MPa data). Conversely, the response to DPI was less in *p5cs1-4*, indicating that Pro synthesis via P5CS1 was required for DPI-induced Pro accumulation. At low ψ_w,

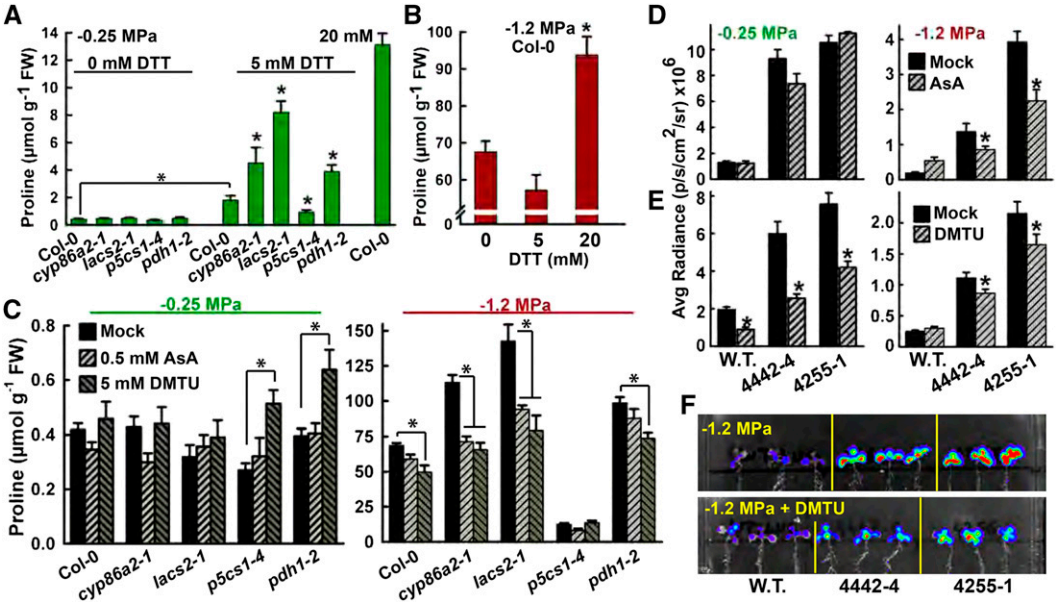

Figure 5. Effects of DTT and the ROS scavengers AsA and DMTU on Pro accumulation and *PDH1*$_{pro}$:*LUC2* activity. A, Effects of DTT treatment on the Pro accumulation of seedlings at high ψ_w. FW, Fresh weight. Data are means ± SE (n = 10–44) combined from three experiments. Significant differences ($P \geq 0.05$) compared with the wild type in the same treatment or between 0 and 5 mM DTT treatment of the wild type are marked with asterisks. B, Effects of DTT treatment at −1.2 MPa on Pro accumulation. Data are means ± SE (n = 10–44) combined from three experiments. Significant differences ($P \geq 0.05$) compared with the wild type are marked with asterisks. C, Effects of AsA and DMTU on Pro levels at −0.25 and −1.2 MPa. Data are means ± SE (n = 10–44) combined from three experiments. Significant differences ($P \geq 0.05$) compared with the mock treatment are marked with asterisks. D, Effects of AsA on *PDH1*$_{pro}$:*LUC2* activity in the wild type, 4442-4, and 4255-1 at high ψ_w (−0.25 MPa) or low ψ_w (−1.2 MPa). Data are means ± SE (n = 10–44) combined from three experiments. Significant differences ($P \geq 0.05$) compared with the mock treatment are marked with asterisks. E, Effects of DMTU on *PDH1*$_{pro}$:*LUC2* activity in the wild type, 4442-4, and 4255-1. Data are means ± SE (n = 10–44) combined from three experiments. Significant differences ($P \geq 0.05$) compared with the mock treatment are marked with asterisks. Luminescence intensities in D and E are given in photons (p) per second (s) per cm^2 per steradian (sr). F, False-color imaging of *PDH1*$_{pro}$:*LUC2* activity in representative seedlings from the experiments reported in E.

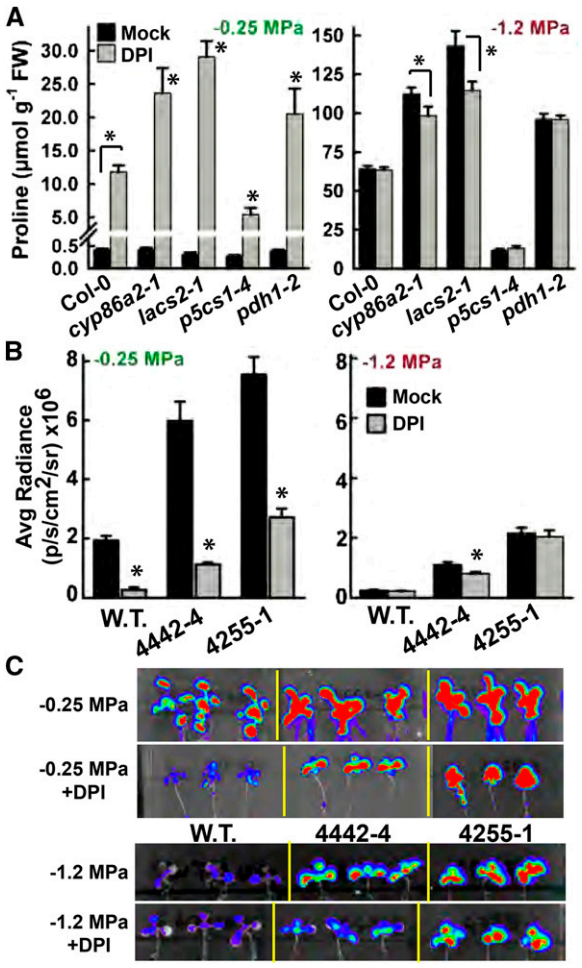

Figure 6. Effects of DPI on Pro accumulation and *PDH1*$_{pro}$*:LUC2* activity. A, Effects of DPI (2.5 μM) on Pro accumulation of seedlings at high ψ_w (−0.25 MPa) or low ψ_w (−1.2 MPa). FW, Fresh weight. Data are means ± SE (n = 14–18) combined from three experiments. Significant differences ($P \geq 0.05$) compared with the wild type (Col-0) in the same treatment or between mock and DPI treatments of Col-0 are marked with asterisks. B, Effects of DPI on *PDH1*$_{pro}$*:LUC2* activity in the wild type (W.T.), 4442-4, and 4255-1 at high ψ_w (−0.25 MPa) or low ψ_w (−1.2 MPa). Data are means ± SE (n = 10–44) combined from three experiments. Significant differences ($P \geq 0.05$) compared with the mock treatment are marked with asterisks. Luminescence intensities are given in photons (p) per second (s) per cm^2 per steradian (sr). C, False-color imaging of *PDH1*$_{pro}$*:LUC2* activity in representative seedlings from the experiments reported in B.

where Pro levels are already high and *PDH1*$_{pro}$*:LUC2* expression is lower, DPI had a lesser effect (Fig. 6, A and B).

Despite the DPI data, measurements of NADP$^+$-NADPH ratio found no significant differences between the wild type, *cyp86a2*, and *lacs2-1* (Supplemental Fig. S5). There was an accumulation of NADPH in all genotypes at low ψ_w, consistent with previous data (Sharma et al., 2011); however, we did not find a significant difference in the NADP$^+$-NADPH ratio. We also did not see any differences in the amount or localization of ROS staining between the wild type, *cyp86a2-1*, and *lacs2-1* (Supplemental Fig. S6), indicating that uncontrolled ROS buildup did not occur under our stress conditions. These assays do not rule out the involvement of NADP$^+$-NADPH ratio, increased ROS, or ROS signaling in the *cyp86a2* and *lacs2-1* phenotypes. However, when combined with the AsA, DMTU, and DPI data, these measurements do suggest that any changes in ROS or pyridine nucleotide redox status may be specific to certain subcellular compartments. This is perhaps consistent with changes in VLCFA synthesis in the endoplasmic reticulum being communicated to Pro metabolism in the cytoplasm and mitochondria by specific, but unknown, signaling mechanisms. In this way, redox status may be buffered before damaging bulk changes in redox metabolites or ROS occur. The redox status of the chloroplast also is very likely to be involved in such redox communication and also may influence Pro accumulation (see below).

RNA Sequencing of *p5cs1-4* Shows the Influence of Pro Synthesis on the Redox Metabolism of Chloroplast and Mitochondria

To further test the relationship between Pro- and redox-related metabolism, as well as more generally investigate the effects of reduced Pro synthesis, mRNA sequencing of *p5cs1-4* was conducted. *p5cs1-4* lacks P5CS1 protein expression (Fig. 4A) and has greatly reduced Pro accumulation and reduced growth at low ψ_w (Székely et al., 2008; Sharma et al., 2011; Kesari et al., 2012; Bhaskara et al., 2015). For the Col-0 wild type, RNA sequencing (Fig. 7A; Supplemental Table S1) found 1,232 genes with significantly increased expression at low ψ_w, with an enrichment of GO terms associated with abiotic stress (Supplemental Table S2). Conversely, 1,155 genes were down-regulated (Supplemental Table S3). As one way to assess the quality of this data set, we compared it with microarray data from Bhaskara et al. (2012), who used the same 96-h, −1.2-MPa stress treatment. Approximately half the genes found to be stress up- or down-regulated in Col-0 by RNA sequencing also were found to be up- or down-regulated in the microarray analysis of Bhaskara et al. (2012; Fig. 7B). This is a substantial overlap between the two data sets, when one considers that the RNA sequencing analysis detects genes not present on the ATH1 chips used by Bhaskara et al. (2012) and that, for high-expression genes, RNA sequencing can be more effective in detecting small changes in expression. Conversely, even large fold-change expression differences of genes with overall low expression (low read counts) did not pass the statistical cutoffs used in analyzing the RNA sequencing data.

For *p5cs1-4*, 111 genes were significantly up-regulated and 132 were down-regulated compared with wild-type Col-0 in the unstressed high-ψ_w treatment. At low ψ_w, 61 genes were significantly up-regulated and 106 genes were down-regulated in *p5cs1-4* compared with wild-type Col-0 (Fig. 7, B and D; Supplemental Tables S4–S7). There were three main patterns of interest in the *p5cs1-4* gene expression data. The most prominent pattern was that genes differentially expressed in *p5cs1-4* were

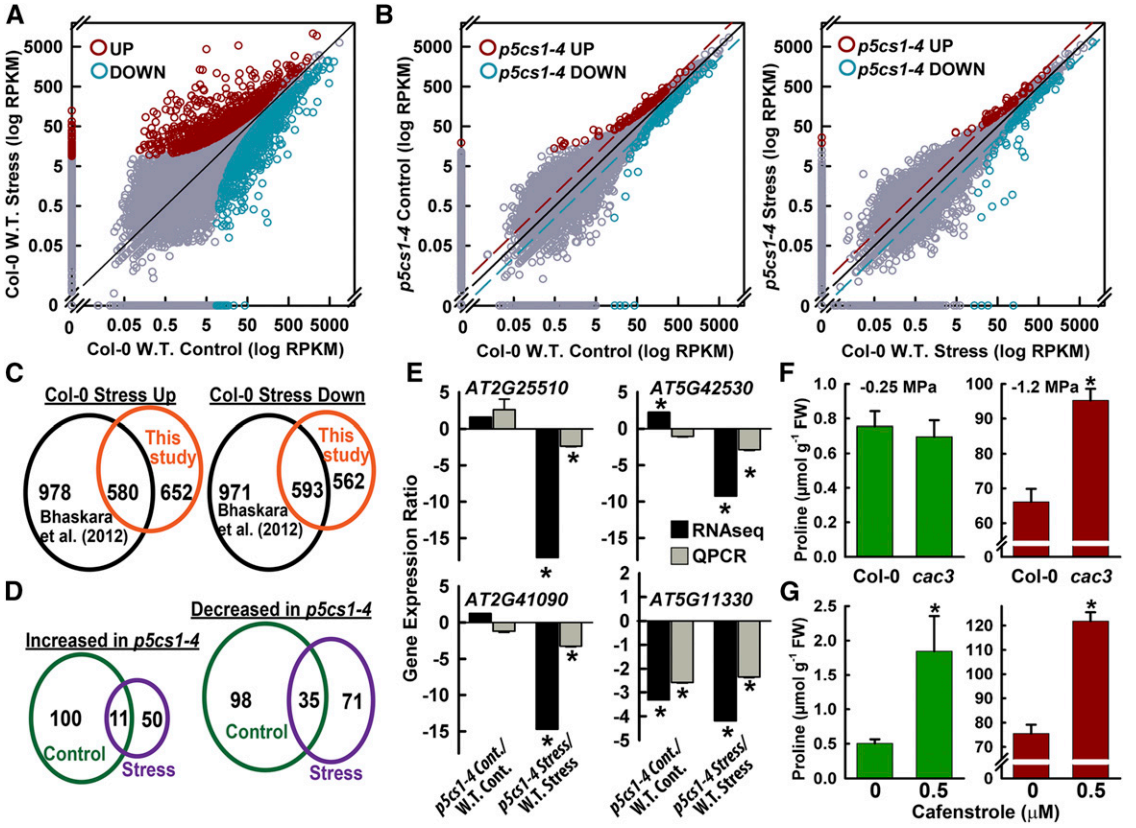

Figure 7. RNA sequencing of the Col-0 wild type (W.T.) and *p5cs1-4* shows the effects of Pro on chloroplast and mitochondria metabolism and identifies additional lipid metabolism loci affecting Pro accumulation. A, Plot of reads assigned per kilobase of target per million mapped reads (RPKM) values for Col-0 in the unstressed control versus Col-0 after 96 h of low-ψ_w (−1.2 MPa) treatment. Significantly up- or down-regulated genes are indicated by red or blue circles, respectively, while other data points are plotted in gray. A complete listing of RPKM values can be found in Supplemental Table S1, and lists of significantly up- or down-regulated genes as well as significantly enriched Gene Ontology (GO) terms can be found in Supplemental Tables S2 and S3. B, Plots of RPKM values for *p5cs1-4* versus the Col-0 wild type in the unstressed control treatment and after 96 h of low-ψ_w treatment. Data presentation is as described for A. A complete listing of RPKM values can be found in Supplemental Table S1, and lists of significantly up- or down-regulated genes in *p5cs1-4* in both control and stress treatments along with a listing of significantly enriched GO terms can be found in Supplemental Tables S4 to S7. Dashed lines indicate two-fold difference in RPKM. C, Comparison of low-ψ_w up- or down-regulated genes identified by RNA sequencing with those identified by previous microarray analysis of the same stress treatment. D, Comparison of genes up- or down-regulated in *p5cs1-4* in the control and low-ψ_w stress treatments. E, Comparison of fold change in gene expression detected by RNA sequencing versus fold change detected by quantitative PCR (qPCR) for selected genes down-regulated in *p5cs1-4*. qPCR data are means ± SE ($n = 5–6$) from two experiments. Ratios significantly different ($P \geq 0.05$) from 1 based on a one-sided Student's *t* test are indicated with asterisks. F, Pro levels in unstressed control treatment (−0.25 MPa) or after 96 h of low-ψ_w treatment (−1.2 MPa) for the Col-0 wild type and the *cac3* mutant. FW, Fresh weight. Data are means ± SE ($n = 15–18$) from three experiments. A significant difference ($P \geq 0.05$) compared with the wild type in the same treatment is marked with an asterisk. G, Effects of the KCS inhibitor cafenstrole on Pro accumulation at high or low ψ_w. Data are means ± SE ($n = 15–18$) from three experiments. Significant differences ($P \geq 0.05$) compared with the wild type in the same treatment are marked with asterisks.

strongly enriched for functions in chloroplast and mitochondrial redox metabolism (see significantly enriched GO categories in Supplemental Tables S4–S7). This included a striking prevalence of chloroplast-encoded genes among the genes having higher expression in unstressed *p5cs1-4* (14 chloroplast-encoded genes out of 111 genes significantly up-regulated; Supplemental Table S4). The portion of chloroplast genes up-regulated in unstressed *p5cs1-4* was significantly higher (enriched) compared with the portion of chromosome-encoded genes (two-tailed $P < 1 \times 10^{-16}$ by Fisher's exact test). The genes up-regulated in *p5cs1-4* at low ψ_w also had a significant enrichment of chloroplast-encoded genes (seven out of 61 up-regulated genes; Supplemental Table S6; two-tailed $P < 1 \times 10^{-8}$ by Fisher's exact test). In unstressed *p5cs1-4*, the majority of the most highly up-regulated genes (greater than 5-fold) were chloroplast-encoded genes (Supplemental Table S4). The effects of *p5cs1-4* on photosynthesis gene expression were concentrated in the light reactions, while there was little effect of

p5cs1-4 on Calvin cycle- or photorespiration-related genes (MapMan analysis; Supplemental Fig. S7). In addition to these genes up-regulated in *p5cs1-4*, GO analysis found strong and statistically significant enrichment of photosynthesis-related functions among the genes down-regulated in *p5cs1-4* (Supplemental Tables S5 and S7).

Also striking was the observation that more than 30 genes encoding chloroplast or mitochondrial NAD(P)H dehydrogenases, as well as genes involved in splicing or processing mitochondrial NAD genes, had higher RPKM values in *p5cs1-4*, while only three such genes had lower RPKM in *p5cs1-4* (Supplemental Table S10; note that this analysis included all genes with fold change greater than 2 to include genes with large fold changes that could not be called significant changes because of low read counts in the wild type). MapMan analysis also showed that *p5cs1-4* had a notably different expression pattern of genes encoding mitochondrial function genes, particularly genes in electron transport complex I, compared with the wild type (Supplemental Fig. S8). Also, *p5cs1-4* had altered expression of a number of other oxidation reduction-related genes of less clear function (such as At5g11330; Fig. 7E). Together, these data indicate substantially altered chloroplast and mitochondrial electron transport in *p5cs1-4* at both high and low ψ_w.

The second pattern of interest was the overall similar numbers of genes and similar GO enrichment profiles of up- or down-regulated genes in *p5cs1-4* for both control and stress treatments (Supplemental Tables S4–S7). There were differences in the individual genes significantly increased or decreased by *p5cs1-4* in control and stress treatments (Fig. 7D). This may be mainly a stochastic effect, as many genes narrowly missed our statistical cutoff in either the control or stress treatment. The genes up- or down-regulated in *p5cs1-4* included both genes whose expression was affected by stress in the wild type and further altered in *p5cs1-4* as well as genes with altered expression in *p5cs1-4* but not affected by low ψ_w in the wild type (Supplemental Tables S8 and S9).

The third pattern of interest was the relative absence of amino acid and nitrogen metabolism functions among genes differentially expressed in *p5cs1-4*. The most strongly enriched GO terms in *p5cs1-4* up- or down-regulated genes did not include any terms related to amino acid or nitrogen metabolism (Supplemental Tables S4–S7; GO terms with $P \leq 0.001$). Only a few GO terms related to Glu metabolism, ammonia transport, or ammonia assimilation were found, and these were overall less highly enriched (Supplemental Tables S4–S7), and the number of genes represented in these categories was dwarfed by the number of genes in other functional categories. Even when all the genes with 2-fold or greater RPKM differences between *p5cs1-4* and the wild type were included, MapMan analysis showed that very few genes mapped to amino acid and nitrogen metabolism pathways compared with greater numbers of genes in chloroplast light reactions and mitochondrial electron transport (Supplemental Fig. S9). These observations are consistent with the conclusions of Less and Galili (2008), who found that transcriptional regulation of Pro metabolism differed from that of other amino acid metabolism pathways. Thus, the *p5cs1-4* transcriptome analysis, as well as the *cyp86a2* and *lacs2* mutant experiments described above, indicated that Pro metabolism is coordinated extensively with cellular redox status. This included chloroplast and mitochondrial electron transport as well as lipid metabolism. At the same time, the data indicated much less connection of Pro to other aspects of carbon-nitrogen metabolism.

We also used the Signature tool in Genevestigator to find publicly available microarray data with similar patterns of differentially expressed genes to *p5cs1-4* under either control or stress conditions. For *p5cs1-4* in the unstressed control treatment, this analysis found several data sets related to light signaling (*phyA* and *cop1* mutants) or different light treatments as well as salicylic acid (SA) treatment (Supplemental Fig. S10). For *p5cs1-4* at low ψ_w, there was similarity to gene expression changes observed in SA synthesis and signaling mutants (e.g. *sid2-1*, *npr1*, and *ssi2*) as well as other pathogen signaling mutants (Supplemental Fig. S11). The similarities between *p5cs1*-affected and light-affected gene expression were consistent with the relationship to chloroplast and photosynthesis gene expression described above. The similarities to pathogen- and SA-related gene expression were consistent with recent data on the role of Pro metabolism in pathogen resistance (Cecchini et al., 2011; Senthil-Kumar and Mysore, 2012). However, it should be noted that these similarities in gene expression were somewhat limited, and *p5cs1-4* had an overall pattern of gene expression that was distinct from any of the data sets included in the Genevestigator analysis.

p5cs1-4 mRNA Sequencing Identifies Additional Lipid Metabolism Genes That Influence Pro Accumulation

Given our findings of altered Pro accumulation in *cyp86a2* and *lacs2-1* mutants, we searched the *p5cs1-4* RNA sequencing data for genes related to VLCFAs, cuticle or wax synthesis, or other genes related to fatty acid metabolism that had different read counts in *p5cs1-4* compared with the wild type (Supplemental Table S11). Interestingly, *ACCD* (Atcg00500), which encodes a subunit of the acetyl-CoA carboxylase complex responsible for the first step of fatty acid synthesis in plastids (Li-Beisson et al., 2013), had 14-fold higher RPKM in stressed *p5cs1-4* compared with the wild type (this difference was marginally nonsignificant in our statistical analysis). The acetyl-coenzyme A carboxylase (ACC) complex consists of several nucleus-encoded subunits in addition to the chloroplast-encoded ACCD. We isolated a T-DNA mutant of the nucleus-encoded ACC α-subunit (*CAC3*; At2g38040) as a way to decrease the activity of the ACC complex. The *cac3* mutant had a nearly 30% increase in Pro accumulation at low ψ_w (Fig. 7F).

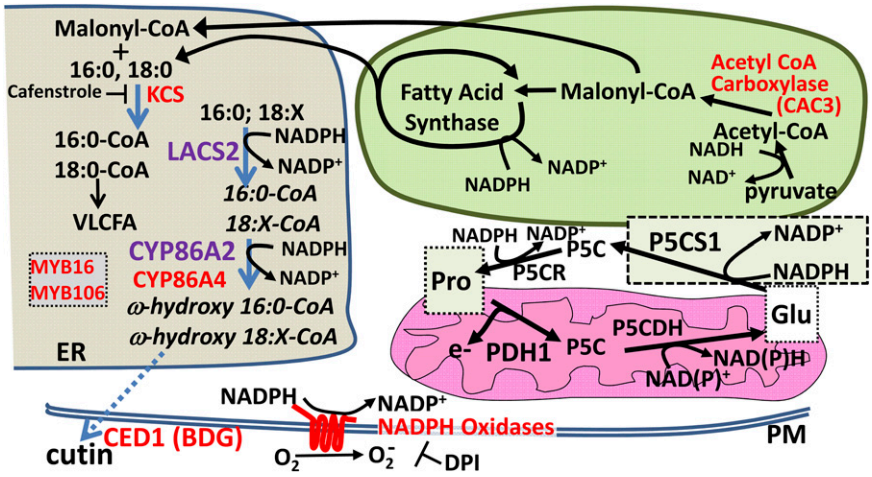

Figure 8. Summary diagram showing the core pathway of Pro metabolism in relation to lipid, cuticle, and redox-related genes found to affect Pro accumulation. Multiple genes and pharmacological treatments disrupting lipid metabolism or NADPH oxidase activity were found to affect Pro accumulation and *PDH1*$_{pro}$*:LUC2* expression. This included *CYP86A2* and *LACS2* identified in the *PDH1*$_{pro}$*:LUC2* forward genetic screen; *CYP86A4*, *CED1*, *MYB16*, and *MYB106* identified by reverse genetics; *CAC3* and *KCS* genes identified by *p5cs1-4* RNA sequencing; as well as strong effects of the NADPH oxidase inhibitor DPI. The reactions catalyzed by these proteins are spread across several compartments, including endoplasmic reticulum (ER), chloroplast, and plasma membrane (PM). The commonality among these pathways and Pro metabolism itself is an effect on redox status by the consumption of NADPH and the regeneration of $NADP^+$, either directly, as for P5CS1, P5CR, LACS2, CYP86A2, and NADPH oxidases, or indirectly by modifying the flux through lipid synthesis, as for CAC3, KCS, CED1, MYB16, and MYB106. This commonality, along with data obtained with ROS scavengers and DTT treatment, indicates that redox status is a key factor linking these pathways together. Consistent with this, RNA sequencing data showed that *p5cs1-4* had substantial alterations in gene expression-related chloroplast and mitochondrial redox metabolism, further indicating the relationship of Pro to redox status. The similar effects of *p5cs1-4* on gene expression at both high and low ψ_w indicated the importance of Pro metabolism, and likely a high rate of flux through the Pro cycle of synthesis and catabolism, even in unstressed plants where Pro level is low. P5CS1 is drawn in its own box to indicate that its subcellular localization is unclear. How changes in redox state are communicated between these subcellular compartments is unknown.

RPKM differences also were found for several genes encoding 3-ketoacyl-coenzyme A synthases (*KCS*). In this case, the fact that several *KCS* genes had putatively altered expression (Supplemental Table S11) suggested that functional redundancy may mask phenotypes of single *kcs* mutants. Instead, we used the KCS inhibitor cafenstrole, which has been shown to block KCS activity (Trenkamp et al., 2004; Nobusawa et al., 2013). Cafenstrol treatment increased the Pro content of unstressed seedlings nearly 3-fold and increased Pro accumulation at low ψ_w by more than 40% (Fig. 7G). Both KCS and the ACC complex act upstream or in a different branch of VLCFA metabolism compared with LACS2 and CYP86A2. Thus, these results added further evidence that blocking flux through lipid metabolism at any of a number of steps leads to increased Pro accumulation at low ψ_w. The *cac3* and cafenstrole data also indicated that the buildup of lipid metabolism intermediates upstream of LACS2 was not responsible for the high-Pro phenotypes of *cyp86a2-1* and *lacs2-1*.

DISCUSSION

We present two major lines of evidence that show how Pro metabolism is integrated into cellular metabolism, particularly the relationship of Pro to lipid metabolism and the relationship to redox metabolism of mitochondria and chloroplast. First, *cyp86a2* and *lacs2-1*, as well as disruptions of lipid metabolism or transport at other points (ACC complex, KCS, CED1, CYP86A4, MYB16, and MYB106), all led to increased Pro accumulation at low ψ_w (summarized in Fig. 8). The high-Pro and high-*PDH1*$_{pro}$*:LUC2* phenotypes of *cyp86a2* and *lacs2-1* could be partially or completed abolished by treatment with ROS scavengers. Similarly, *cyp86a2-1* and *lacs2-1* were more sensitive to the activation of Pro accumulation by reductant (DTT) or inhibited NADPH oxidase activity (DPI). Together, these data indicated that an effect of altered VLCFA synthesis on redox status, rather than signaling function of CYP86A2, LACS2, or VLCFAs themselves, was the cause of increased *PDH1*$_{pro}$*:LUC2* expression and Pro accumulation. In a complementary line of experiments, we discovered that disrupted Pro synthesis in *p5cs1-4* altered the expression of chloroplast and mitochondrial genes related to redox metabolism. Two main conclusions emerge from these data. The first is that Pro metabolism is both influenced by and influences cellular redox status via previously unknown coordination with multiple metabolic pathways. A second conclusion is that Pro and lipid metabolism share dual roles under stress to help buffer cellular redox status while producing Pro and cuticle lipids useful for drought tolerance.

We selected the *PDH1* promoter for forward genetic screening because it could serve as a sensor for alterations in both stress signaling and metabolic state. Both *cyp86a2* (4442-4) and *lacs2* (4255-1) mutants had increased $PDH1_{pro}$:*LUC2* expression, but not increased Pro, in the unstressed control. In the wild-type background, $PDH1_{pro}$:*LUC2* expression of unstressed seedlings could be fully repressed to the stress level simply by the addition of the NADPH oxidase inhibitor DPI. The high $PDH1_{pro}$:*LUC2* expression of *cyp86a2* and *lacs2* mutants likewise could be repressed by DPI. Together, these data show that $PDH1_{pro}$:*LUC2* indeed acted as a sensitive indicator of altered redox and metabolic state even under conditions where Pro level itself was not changed. At low ψ_w, DPI, AsA, and DMTU had lesser, but still significant, effects, presumably because other stress-related signals also were acting on $PDH1_{pro}$:*LUC2* expression and Pro accumulation. The $PDH1_{pro}$:*LUC2* system can be further used as a new tool to understand unknown redox, metabolic, and stress signaling mechanisms.

It was of interest that there was not a complete correspondence between the expression of the $PDH1_{pro}$:*LUC2* reporter and endogenous *PDH1* at low ψ_w. The two agreed very well in unstressed plants. At low ψ_w, however, the endogenous *PDH1* was fully repressed despite the high Pro accumulation in *cyp86a2* and *lacs2*, while the $PDH1_{pro}$:*LUC2* reporter was only partially repressed. It is possible that the $PDH1_{pro}$:*LUC2* construct may not incorporate all elements (such as the 3′ UTR or *PDH1* coding region) responsible for the stress repression of *PDH1*. Alternatively, there may be position-dependent regulation of the *PDH1* promoter that does not occur at the $PDH1_{pro}$:*LUC2* locus. While fortuitous, this partial decoupling of *PDH1* and $PDH1_{pro}$:*LUC2* at low ψ_w allowed a larger range of mutants affecting Pro accumulation to be isolated. The $PDH1_{pro}$:*LUC2* system, and modifications of it that include more or differing sections of *PDH1*, can be used as a system to explore the stress repression of *PDH1* more fully.

The *cyp86a2* and *lacs2* mutants had altered Pro accumulation despite no difference in P5CS1 or PDH1 protein level or any change in expression of the core Pro metabolism genes. How Pro and VLCFA metabolism are coordinated is part of a larger question of how redox state can be communicated between different subcellular compartments such as the endoplasmic reticulum, chloroplast, and mitochondria. Such mechanisms are little known, and Pro metabolism is a promising system in which to address such questions. However, we must first more definitively answer fundamental questions, such as where Pro is synthesized (cytoplasm or chloroplast). It is also interesting that mutants of *PDH1*, *CYPP86A2*, and *LACS2* all have pathogen resistance phenotypes (Xiao et al., 2004; Bessire et al., 2007; Cecchini et al., 2011; Senthil-Kumar and Mysore, 2012). Also, there were similarities between genes differentially expressed in *p5cs1-4* and genes differentially expressed in defense signaling and SA-related mutants (Supplemental Figs. S10 and S11). For *pdh1* mutants, their altered pathogen resistance is due to Pro- and PDH1-dependent mitochondrial ROS production. Possibly, altered Pro levels and redox status are involved in the pathogen resistance phenotypes of *cyp86a2* and *lacs2* and are at least partially responsible for the gene expression changes in *p5cs1-4*.

RNA sequencing of *p5cs1-4* further supported the coordination of Pro and lipid metabolism and showed a striking effect of *p5cs1-4* on the expression of genes involved in redox metabolism of the mitochondria and chloroplast. These results are consistent with those of Lovell et al. (2015), who conducted quantitative trait locus mapping using a recombinant inbred line population constructed using Arabidopsis accessions Tsu and Kas, which have contrasting levels of Pro accumulation during drought. They found a significant cytoplasmic effect on Pro accumulation, and the most likely variation underlying this affect was in mitochondrial *NADH Dehydrogenase Subunit9* (*NAD9*). In our data, *NAD9* had 10-fold higher RPKM in *p5cs1-4* compared with the wild type at high ψ_w and 3-fold higher at low ψ_w (Supplemental Table S10). In addition, more than 15 other *NAD*s and related genes had similar patterns of higher RPKM in *p5cs1-4* (Supplemental Table S10). It is possible that *NAD* expression is up-regulated to compensate for the reduced Pro level (and presumably reduced Pro catabolism) in *p5cs1-4*. These data underscore the importance of the Pro cycle to feed reductant into the mitochondria and are consistent with other evidence showing the importance of mitochondrial metabolism in drought resistance (Pastore et al., 2007; Giraud et al., 2008; Zsigmond et al., 2008; Atkin and Macherel, 2009; Rasmusson and Wallström, 2010; Skirycz et al., 2010; Schertl et al., 2014).

Under both high and low ψ_w, there was a striking enrichment of chloroplast-encoded genes among genes differentially expressed in *p5cs1-4*. This included genes involved in chloroplast protein translation as well as genes involved directly in the light reactions and NADPH metabolism. How and why disrupting Pro metabolism had such a striking effect on chloroplast gene expression is not as immediately clear as the connection of Pro to mitochondrial metabolism. However, the gene expression differences we saw in *p5cs1-4* are broadly consistent with the idea that Pro metabolism may have a role in consuming NADPH and regenerating $NADP^+$ to provide a continued supply of electron acceptors for chloroplast electron transport (Sharma et al., 2011) and with observations that Pro accumulation and Pro metabolism gene expression are modulated by light (Hayashi et al., 2000; Abrahám et al., 2003). The fact that effects of *p5cs1-4* on chloroplast gene expression could be seen even in unstressed plants implies that flux through the cycle of Pro synthesis and catabolism is high enough to impact chloroplast function even when Pro levels are low. Further interpretation of these data is limited by the dearth of knowledge of metabolic flux through Pro metabolism, the unclear subcellular localization of P5CS1, and the lack of data on whether Pro metabolism mutants have reduced photosynthetic efficiency. In chloroplasts, enzyme activities are coordinated with redox status via the modification of protein disulfide bond status by

ferredoxins and thioredoxins (Meyer et al., 2012). It will be of interest to further investigate how redox metabolism in the chloroplast could be coordinated with Pro synthesis that likely (although not certainly) occurs in the cytoplasm. Likewise, it has been suggested the mammalian P5CS may be regulated by thioredoxins (Liang et al., 2013). Whether similar regulation exists in plants has not been investigated, to our knowledge. Our *p5cs1-4* transcriptome data make further experiments to uncover the specific mechanisms underlying the redox-Pro and Pro-photosynthesis connections even more compelling.

To our knowledge, there are little or no data directly comparable to our transcriptome analysis of *p5cs1-4*. Perhaps the most closely related work is that of Satoh et al. (2002), who reported genes induced by exogenous Pro. We may expect that these genes would be less expressed in stressed *p5cs1-4*, which has greatly decreased Pro levels compared with the wild type. Indeed, five out of the 20 Pro-inducible genes with a ProRE reported by Satoh et al. (2002) were less expressed in *p5cs1-4* (Supplemental Table S8); however, three such genes were up-regulated in *p5cs1-4* (Supplemental Table S9). Satoh et al. (2002) also found other genes responsive to Pro but lacking a ProRE. However, the identity of these genes was not reported, precluding further comparison with our data. Whether *PDH1* and the ProRE are regulated directly by Pro level via some unknown Pro-sensing mechanism or respond indirectly to other metabolic or redox-related signaling factors, as suggested by our analysis of *cyp86a2* and *lacs2* mutants, will be a question of interest as we characterize additional mutants from the $PDH1_{pro}$:*LUC2* screen.

We observed that the NADPH oxidase inhibitor DPI caused a massive increase in the Pro content of unstressed seedlings and suppressed $PDH1_{pro}$:*LUC2* expression in the wild type as well as in *cyp86a2* and *lacs2* mutants. These data indicate how redox status, possibly including the redox status of the NADPH pool or ROS signaling, may be involved in adjusting Pro metabolism to match cellular redox and metabolic state. However, our result differs from that of Ben Rejeb et al. (2015), who saw no effect of DPI on the Pro accumulation of unstressed plants. Their experiments were conducted on medium containing Suc, which could have altered metabolite levels and redox status and thus obscured the DPI Pro response.

The hypothesis that Pro metabolism is regulated by redox or metabolic factors as well as abiotic stress has been proposed and discussed in several places (Szabados and Savouré, 2010; Verslues and Sharma, 2010; Sharma et al., 2011; Servet et al., 2012; Liang et al., 2013; Ben Rejeb et al., 2014; Giberti et al., 2014; Zhang and Becker, 2015), but experimental data to support such hypotheses are limited. The $PDH1_{pro}$:*LUC2* mutant screen has revealed an unexpected coordination of Pro and lipid metabolism, with altered cellular redox status being one of the factors allowing the coordinated regulation of these pathways. Likewise, the gene expression data set reported here greatly strengthens hypotheses that the Pro cycle is a significant determinant of chloroplast and mitochondria metabolism even when the Pro level is low. Our study demonstrates the need to mechanistically understand the redox-dependent regulation of Pro metabolism. For example, do Pro metabolism proteins undergo redox-sensitive posttranslational modifications that affect their activity, or does the transcriptional regulation of *PDH1* transcription include redox-sensitive factors? The $PDH1_{pro}$:*LUC2* screen and the characterization of additional mutants promise to provide further new insights into Pro metabolism, its regulation, and its roles in stress resistance.

MATERIALS AND METHODS

Construction of $PDH1_{pro}$:*LUC2*, Mutagenesis, and Screening

A 1,511-bp fragment encompassing the *PDH1* promoter out to −1,389 bp and the 5′ UTR (122 bp) of the Arabidopsis (*Arabidopsis thaliana*) PDH1 transcript was amplified using primers to add *Pst*I and *Sal*I cloning sites (primer sequences are given in Supplemental Table S12). This promoter fragment was chosen because it was similar in length to the *PDH1* promoter fragment we used previously to analyze *PDH1* promoter:GUS expression (Sharma et al., 2011) and contains the ProRE described by Satoh et al. (2002) as well as several other potential cis-elements (Nakashima et al., 1998). This fragment was 112 bp shorter than the *PDH1* promoter fragment we used previously for promoter:GUS analysis (Sharma et al., 2011) to avoid a *Sal*I site that interfered with cloning. The amplified fragment was ligated into pJET1.2 blunt cloning vector (Thermo Fisher Scientific) and confirmed by sequencing. The *PDH1* promoter fragment was then cloned into pCAB2-LUC2-pCAMBIA1390 (Wang et al., 2011a) containing the pGL4.10-LUC2 (Promega) Luciferase2 sequence. pCAB2-LUC2-pCAMBIA1390 was *Sal*I/*Pst*I digested and gel purified to remove the CAB2 promoter and then ligated with the *Pst*I-*PDH1* promoter-*Sal*I fragment. The resulting plasmid was transformed into *Agrobacterium tumefaciens* strain GV3101 by electroporation and used to transform the Col-0 wild type by the floral dip method. T2 lines having a 3:1 segregation ratio consistent with a single-locus insertion were selected, and homozygous T3 plants were confirmed by antibiotic screening. These lines were further tested for similar repression of $PDH1_{pro}$:*LUC2* during low ψ_w and the induction of $PDH1_{pro}$:*LUC2* expression upon stress release as the endogenous *PDH1*. A single transgenic line was selected for mutagenesis. Subsequent genome sequencing confirmed that this line has insertion of the $PDH1_{pro}$:*LUC2* construct adjacent to position 11,887,500 of chromosome 1.

Approximately 60,000 T3 seeds of this line were EMS mutagenized following standard protocols (Weigel and Glazebrook, 2006). Mutagenized seeds were sown in large pots (approximately 60–70 seed per pot). M1 seeds from each pot were collected together as a pool, resulting in more than 900 pools of mutagenized seeds. From each of these pools, 100 seeds were sterilized and plated in a grid pattern on 140-mm-diameter plates on which the agar had been overlaid with nylon mesh to facilitate seedling transfer. The medium used was our laboratory standard medium of one-half-strength Murashige and Skoog salts with 2 mM MES (pH 5.7) buffer but no sugar (Sharma et al., 2011). Each plate also included three to five unmutagenized $PDH1_{pro}$:*LUC2* seeds for comparison. After stratification for 4 d, plates were incubated vertically in a growth chamber (23°C and light intensity of 100 μmol m^{-1} s^{-1}) for 7 d. On day 7, plates were sprayed with 1 mM luciferin and imaged using a Xenogen Ivis system (Perkin-Elmer). Seedlings having high or low luciferase activity were marked. Seedlings were then transferred to low-ψ_w polyethylene glycol (PEG)-infused agar plates (−1 MPa) for 4 d, and luciferase activity was imaged again. PEG-agar plates were prepared as described previously (Sharma et al., 2011), with the relative volumes of agar and PEG overlay adjusted for the larger plates.

Seedlings having high or low luciferase activity either before or after the stress treatment were transferred to soil. Seeds from these plants (M2 generation) were then used for a secondary screen conducted in the same manner but with five to eight seedlings per line imaged and luciferase activity quantified (using the Xenogen Ivis software). Several hundred putative mutants were rescreened in the M2 generation, and more than 30 lines with consistently high $ProDH1_{pro}$:*LUC2* activity and a smaller set of mutants with low $ProDH1_{pro}$:*LUC2* (approximately seven, although some are still being verified) were selected for further analysis. Mutants having the greatest difference in luciferase activity compared with the wild type were selected for further analysis, including backcrosses, complementation testing, crosses to Landsberg *erecta* for mapping, and further phenotypic analysis.

Whole-Genome Sequencing, Single-Nucleotide Polymorphism Calling, and Next-Generation Mapping

Mutants having high $PDH1_{pro}$:*LUC2* were crossed to Landsberg *erecta*, and the resulting F2 seeds were plated as described above. Mutants in which the high-$PDH1_{pro}$:*LUC2* phenotype segregated in a 3:1 ratio consistent with a single recessive locus were considered suitable for sequencing analysis (in most cases, the recessive nature of the mutation also was confirmed during backcrossing to unmutagenized $PDH1_{pro}$:*LUC2*). Genomic DNA was extracted from a pool of 80 to 100 homozygous mutant seedlings selected from the F2 population based on their high $PDH1_{pro}$:*LUC2* expression. DNA was extracted using the Qiagen Plant DNeasy kit, and the purity of the DNA extracts was tested by absorbance measurements and agarose gel analysis.

For whole-genome sequencing, six mutant DNA pools were prepared using Illumina TruSeq DNA library construction. Briefly, 1 μg of each DNA pool was sheared to fragments of 150 to 500 bp using a Covaris M220 focused ultrasonicator with the 200-bp program. The sheared DNA was size enriched by double-sided solid-phase reversible immobilization using an Agencourt AmPure XP kit. A TruSeq DNA LT Sample Prep Kit (Illumina) was used to perform end repair, A tailing, and adaptor ligation. The barcoded samples were then amplified by eight cycles of PCR and cleaned up by AmPure XP beads (Beckman Agencourt). The absolute concentrations and profiles of the libraries were determined by Qubit (Invitrogen) and BioAnalyzer High Sensitivity DNA chips (Agilent), respectively. The final library sizes range from 250 to 750 bp, with a major size of 350 bp. The molar concentrations of the libraries were derived by qPCR normalization using the KAPA NGS Library qPCR kit (KAPA Biosystems). Multiplexed sequencing was conducted on one lane of PE2*101 on an Illumina HiSeq2500. The Illumina CASAVA 1.8.2 pipeline was applied for barcode demultiplexing and generating fastq files. The Illuminia sequencing and initial data processing were conducted by the High Throughput Genomics Core facility of the Biodiversity Research Center, Academia Sinica.

After sequencing, reads were mapped to The Arabidopsis Information Resource 10 genome (ftp://ftp.arabidopsis.org/home/tair/Genes/TAIR10_genome_release/) using Bowtie2 (Langmead and Salzberg, 2012) and BLAT (Kent, 2002), and single-nucleotide polymorphism calling was conducted by the RackJ software package (http://rackj.sourceforge.net/). Mapping results in BAM format were processed into pileup files using Samtools version 0.1.16 and then emap files as instructed on the Next Generation Mapping Web site (http://bar.utoronto.ca/NGM/). The processed emap files were analyzed using the Next Generation Mapping analysis tool (http://bar.utoronto.ca/NGM/) described by Austin et al. (2011).

Phenotypic Analyses and T-DNA Mutants

Seeds of T-DNA mutants were obtained from the Arabidopsis Biological Resource Center, and homozygous plants were confirmed by PCR genotyping using primers from the Signal (www.signal.salk.edu) database. RT-PCR was used to confirm the absence of transcript in each new mutant (Supplemental Fig. S12; genotyping and RT-PCR primers are given in Supplemental Table S12). Seeds for *lacs2-1* and *lacs3-1* were provided by the laboratory of Dr. John Browse. The Pro metabolism mutants *p5cs1-4* and *pdh1-2* were verified previously by our laboratory (Sharma and Verslues, 2010; Sharma et al., 2011). For transgenic complementation of 4442-4, the full-length cDNA sequence of *CYP86A2* was amplified from total RNA (primers are given in Supplemental Table S12) and cloned into pDONOR 207. For plant expression, the clone was moved into pEG100 (Earley et al., 2006) and transformed into *A. tumefaciens* GV3101, and the 4442-4 EMS mutant was transformed by the floral dip method.

Free Pro was quantified using a ninhydrin assay (Bates et al., 1973) adapted to 96-well plate format (Verslues, 2010). For pharmacological treatments, seedlings were pretreated with AsA (Sigma), DMTU (ACROS Organics), or DPI (Sigma) for 24 h and then transferred to low ψ_w (−1.2 MPa, 96 h) with the same concentration of the chemical. Cafenstrole (Wako Chemical) treatment was performed in the same manner but without pretreatment before transfer to low ψ_w. Western blotting of P5CS1 and PDH1 was performed using antisera generated by our laboratory as described previously (Kesari et al., 2012; Bhaskara et al., 2015). For Toluidine Blue staining, whole seedlings or leaves were submerged in an aqueous solution of 0.05% (w/v) Toluidine Blue for 2 to 5 min. Excess stain was removed by rinsing with sterile distilled water before being photographed using a Lumar v12 stereoscope (Zeiss). For RT-PCR and quantitative RT-PCR analysis, total RNA was extracted from seedlings using the RNeasy plant mini kit (Qiagen). Quantitative PCR was performed using KAPA SYBR FAST Master Mix on a QuantStudio 12K Flex Real-Time PCR System (Applied Biosystems). NADP and NADPH were measured using an analysis kit (BioAssay Systems) with sample collection and extraction performed as described previously (Sharma et al., 2011). ROS staining used 2′,7′-dichlorodihydrofluorescein diacetate dye with excitation at 488 nm and emission at 500 to 550 nm, with images analyzed on a Zeiss LSM510 Meta microscopy system.

mRNA Sequencing

mRNA sequencing was carried out by the High Throughput Genomics Core facility of the Biodiversity Research Center, Academia Sinica, following the protocols provided by Illumina, including mRNA sequencing library preparation, addition of MID barcodes to the double-stranded cDNA fragments, and volume adjustment. Using the Illumina mRNA-seq kit, 10 to 15 μg of total RNA was used for the isolation of poly(A) RNA by oligo(dT) beads and subjected to cation-catalyzed fragmentation for 4 min at 94°C. The mRNA fragments were then converted into double-stranded cDNA by random priming, and the ends were repaired and A tailed. Multiplexing barcodes were then added to the DNA fragment ends with modifications from the paired-end genomic DNA library prep kit. The ligation products were size selected on agarose gels (200–400 bp), subjected to 18 cycles of PCR, and cleaned up by AmPure beads (Beckman Agencourt). The absolute concentrations of the libraries were determined fluorometrically by Qubit (Invitrogen) and BioAnalyzer High Sensitivity DNA chips (Agilent).

Mixing of the differentially barcoded samples for each lane was based on qPCR-derived relative concentration for the amplifiable fraction of each library. Briefly, the relative amplifiable concentration of each library was estimated by real-time PCR analyses (Roche Light Cycler 480) using the KAPA NGS Library qPCR kit by regression to the curve generated using the included standard of known concentration. Correlations between output clusters and qPCR concentrations were derived by plotting the relative concentrations of previously sequenced PhiX control and libraries against the output cluster numbers. The relative concentrations of the MID libraries were then estimated by regression. The amount (fmol) of each library to be mixed in a pool for each lane was determined based on the proportion each would account for in the projected output clusters (i.e. estimating the fmol required per library to generate 300,000/8 = 37,500 raw clusters per tile if the lane to be used for sequencing contained a pool of eight barcodes). The sequencing was performed on an Illumina Genome Analyzer IIx in the High Throughput Sequencing Core Facility of Academia Sinica, and 73-nucleotide reads were obtained. Base calling and demultiplexing were performed using CASAVA and bclfastq1.6.

RPKM values were calculated using the RackJ software package (http://rackj.sourceforge.net/) with reads mapped to The Arabidopsis Information Resource 10 genome using BLAT (Kent, 2002). RPKM values of control and treatment samples were compared using *Z* statistics as described by Lan et al. (2013). GO enrichment was computed using the TopGO elim method (Alexa et al., 2006) using GOBU with its MultiView plugin (Lin et al., 2006).

Accession Numbers

mRNA sequencing results are available under Gene Expression Omnibus accession number GSE75933.

Supplemental Data

The following supplemental materials are available.

Supplemental Figure S1. Example of primary screen plate images using EMS-mutagenized $PDH1_{pro}$:*LUC2*.

Supplemental Figure S2. Next-generation mapping analysis and identification of *CYP86A2* and *LACS2* as the causative mutated genes in the 4442-2 and 4255-1 EMS mutants.

Supplemental Figure S3. $PDH1_{pro}$:*LUC2* crossed to *cyp86a2-1* and *lacs2-1* T-DNA mutants shows the same high-$PDH1_{pro}$:*LUC2* phenotype as the 4244-2 and 4255-2 EMS mutants.

Supplemental Figure S4. Expression of Pro synthesis and catabolism genes in *cyp86a2* mutants.

Supplemental Figure S5. $NADP^+$ and NADPH analysis of the wild type, *cyp86a2-1*, and *lacs2-1*.

Supplemental Figure S6. ROS levels of the wild type, *cyp86a2-1*, and *lacs2-1*.

Supplemental Figure S7. MapMan analysis of photosynthesis-related gene expression in stress- and control-treated wild-type plants as well as *p5cs1-4* compared with the wild type in unstressed and low-ψ_w (−1.2 MPa, 96 h) treatments.

Supplemental Figure S8. MapMan analysis of mitochondrial electron transport-related gene expression in stress- and control-treated wild-type plants as well as *p5cs1-4* compared with the wild type in unstressed and low-ψ_w (−1.2 MPa, 96 h) treatments.

Supplemental Figure S9. MapMan analysis of amino acid metabolism-related gene expression in *p5cs1-4* compared with the wild type in unstressed and low-ψ_w (−1.2 MPa, 96 h) treatments.

Supplemental Figure S10. Differentially expressed genes in *p5cs1-4* control versus wild-type control compared with public microarray data using the Genevestigator Signature analysis tool.

Supplemental Figure S11. Differentially expressed genes in *p5cs1-4* stress versus wild-type stress compared with public microarray data using the Genevestigator Signature analysis tool.

Supplemental Figure S12. RT-PCR check of lipid- and cuticle-related T-DNA mutants.

Supplemental Table S1. RPKM values from RNA sequencing analysis of wild-type Col-0 and *p5cs1-4* under either control (−0.25 MPa) or stress (transfer to −1.2 MPa for 96 h) conditions.

Supplemental Table S2. Genes with increased expression in the Col-0 wild type at 96 h after transfer to low-ψ_w (−1.2 MPa) stress, and GO terms significantly enriched in the up-regulated genes.

Supplemental Table S3. Genes with decreased expression in the wild type at 96 h after transfer to low-ψ_w (−1.2 MPa) stress, and significantly enriched GO terms among the down-regulated genes.

Supplemental Table S4. Genes with increased expression in unstressed *p5cs1-4* compared with unstressed wild-type Col-0, along with significantly enriched GO terms.

Supplemental Table S5. Genes with decreased expression in unstressed *p5cs1-4* compared with unstressed wild-type Col-0, along with significantly enriched GO terms.

Supplemental Table S6. Genes with increased expression in stressed (−1.2 MPa, 96 h) *p5cs1-4* compared with stressed wild-type Col-0, along with significantly enriched GO terms.

Supplemental Table S7. Genes with decreased expression in stressed (−1.2 MPa, 96 h) *p5cs1-4* compared with stressed wild-type Col-0, along with significantly enriched GO terms.

Supplemental Table S8. Both stress-responsive and nonresponsive genes are among those up-regulated in *p5cs1-4*.

Supplemental Table S9. Both stress-responsive and nonresponsive genes are among those down-regulated in *p5cs1-4*.

Supplemental Table S10. Chloroplast and mitochondrial NAD(P)H dehydrogenase genes with putatively altered expression in *p5cs1-4*.

Supplemental Table S11. Lipid and wax metabolism genes with putatively altered expression in *p5cs1-4*.

Supplemental Table S12. Primer sequences used in this study.

ACKNOWLEDGMENTS

We thank the laboratory of Shu-Hsing Wu for the pCAB2-LUC2-pCAMBIA1390 plasmid; John Browse (Washington State University) for the *lacs2* and *lacs3* mutants; Mei-Yeh Liu and the High Throughput Genomics Core, Biodiversity Research Center, Academia Sinica, for sequencing services; Mei-Jane Fang for assistance with luciferase imaging and microscopy; Ang-Hsi Lin for mutant screening; and Srilakshmi Mukiri and Trent Z. Chang for laboratory assistance.

Received July 14, 2016; accepted August 5, 2016; published August 10, 2016.

LITERATURE CITED

Abrahám E, Rigó G, Székely G, Nagy R, Koncz C, Szabados L (2003) Light-dependent induction of proline biosynthesis by abscisic acid and salt stress is inhibited by brassinosteroid in Arabidopsis. Plant Mol Biol **51:** 363–372

Alexa A, Rahnenführer J, Lengauer T (2006) Improved scoring of functional groups from gene expression data by decorrelating GO graph structure. Bioinformatics **22:** 1600–1607

Atkin OK, Macherel D (2009) The crucial role of plant mitochondria in orchestrating drought tolerance. Ann Bot (Lond) **103:** 581–597

Austin RS, Vidaurre D, Stamatiou G, Breit R, Provart NJ, Bonetta D, Zhang J, Fung P, Gong Y, Wang PW, et al (2011) Next-generation mapping of Arabidopsis genes. Plant J **67:** 715–725

Bates LS, Waldren RP, Teare ID (1973) Rapid determination of free proline for water stress studies. Plant Soil **39:** 205–207

Ben Rejeb K, Abdelly C, Savouré A (2014) How reactive oxygen species and proline face stress together. Plant Physiol Biochem **80:** 278–284

Ben Rejeb K, Lefebvre-De Vos D, Le Disquet I, Leprince AS, Bordenave M, Maldiney R, Jdey A, Abdelly C, Savouré A (2015) Hydrogen peroxide produced by NADPH oxidases increases proline accumulation during salt or mannitol stress in Arabidopsis thaliana. New Phytol **208:** 1138–1148

Bessire M, Chassot C, Jacquat AC, Humphry M, Borel S, Petétot JMC, Métraux JP, Nawrath C (2007) A permeable cuticle in Arabidopsis leads to a strong resistance to Botrytis cinerea. EMBO J **26:** 2158–2168

Bhaskara GB, Nguyen TT, Verslues PE (2012) Unique drought resistance functions of the Highly ABA-Induced clade A protein phosphatase 2Cs. Plant Physiol **160:** 379–395

Bhaskara GB, Yang TH, Verslues PE (2015) Dynamic proline metabolism: importance and regulation in water limited environments. Front Plant Sci **6:** 484

Bussis D, Heineke D (1998) Acclimation of potato plants to polyethylene glycol-induced water deficit. II. Contents and subcellular distribution of organic solutes. J Exp Bot **49:** 1361–1370

Cecchini NM, Monteoliva MI, Alvarez ME (2011) Proline dehydrogenase contributes to pathogen defense in Arabidopsis. Plant Physiol **155:** 1947–1959

de Ronde JA, Cress WA, Krüger GHJ, Strasser RJ, Van Staden J (2004) Photosynthetic response of transgenic soybean plants, containing an Arabidopsis P5CR gene, during heat and drought stress. J Plant Physiol **161:** 1211–1224

Dietrich K, Weltmeier F, Ehlert A, Weiste C, Stahl M, Harter K, Dröge-Laser W (2011) Heterodimers of the *Arabidopsis* transcription factors bZIP1 and bZIP53 reprogram amino acid metabolism during low energy stress. Plant Cell **23:** 381–395

Earley KW, Haag JR, Pontes O, Opper K, Juehne T, Song K, Pikaard CS (2006) Gateway-compatible vectors for plant functional genomics and proteomics. Plant J **45:** 616–629

Funck D, Eckard S, Müller G (2010) Non-redundant functions of two proline dehydrogenase isoforms in Arabidopsis. BMC Plant Biol **10:** 70

Funck D, Winter G, Baumgarten L, Forlani G (2012) Requirement of proline synthesis during Arabidopsis reproductive development. BMC Plant Biol **12:** 191

Giberti S, Funck D, Forlani G (2014) Δ1-Pyrroline-5-carboxylate reductase from Arabidopsis thaliana: stimulation or inhibition by chloride ions and feedback regulation by proline depend on whether NADPH or NADH acts as co-substrate. New Phytol **202:** 911–919

Giraud E, Ho LHM, Clifton R, Carroll A, Estavillo G, Tan YF, Howell KA, Ivanova A, Pogson BJ, Millar AH, et al (2008) The absence of ALTERNATIVE OXIDASE1a in Arabidopsis results in acute sensitivity to combined light and drought stress. Plant Physiol **147:** 595–610

Gleeson D, Lelu-Walter MA, Parkinson M (2005) Overproduction of proline in transgenic hybrid larch (Larix × leptoeuropaea (Dengler)) cultures renders them tolerant to cold, salt and frost. Mol Breed **15:** 21–29

Hayashi F, Ichino T, Osanai M, Wada K (2000) Oscillation and regulation of proline content by P5CS and ProDH gene expressions in the light/dark cycles in Arabidopsis thaliana L. Plant Cell Physiol **41:** 1096–1101

Kavi Kishor PB, Hima Kumari P, Sunita MSL, Sreenivasulu N (2015) Role of proline in cell wall synthesis and plant development and its implications in plant ontogeny. Front Plant Sci **6:** 544

Kent WJ (2002) BLAT: the BLAST-like alignment tool. Genome Res **12:** 656–664

Kesari R, Lasky JR, Villamor JG, Des Marais DL, Chen YJC, Liu TW, Lin W, Juenger TE, Verslues PE (2012) Intron-mediated alternative splicing of Arabidopsis P5CS1 and its association with natural variation in proline and climate adaptation. Proc Natl Acad Sci USA **109:** 9197–9202

Kolbe A, Oliver SN, Fernie AR, Stitt M, van Dongen JT, Geigenberger P (2006) Combined transcript and metabolite profiling of Arabidopsis

leaves reveals fundamental effects of the thiol-disulfide status on plant metabolism. Plant Physiol **141:** 412–422

Lan P, Li W, Lin WD, Santi S, Schmidt W (2013) Mapping gene activity of Arabidopsis root hairs. Genome Biol **14:** R67

Langmead B, Salzberg SL (2012) Fast gapped-read alignment with Bowtie 2. Nat Methods **9:** 357–359

Less H, Galili G (2008) Principal transcriptional programs regulating plant amino acid metabolism in response to abiotic stresses. Plant Physiol **147:** 316–330

Liang X, Zhang L, Natarajan SK, Becker DF (2013) Proline mechanisms of stress survival. Antioxid Redox Signal **19:** 998–1011

Li-Beisson Y, Pollard M, Sauveplane V, Pinot F, Ohlrogge J, Beisson F (2009) Nanoridges that characterize the surface morphology of flowers require the synthesis of cutin polyester. Proc Natl Acad Sci USA **106:** 22008–22013

Li-Beisson Y, Shorrosh B, Beisson F, Andersson MX, Arondel V, Bates PD, Baud S, Bird D, DeBono A, Durrett TP, et al (2013) Acyl-lipid metabolism. The Arabidopsis Book **11:** e0161 doi/10.1199/tab.0161

Lin WD, Chen YC, Ho JM, Hsiao CD (2006) GOBU: toward an integration interface for biological objects. J Inf Sci Eng **22:** 19–29

Lovell JT, Mullen JL, Lowry DB, Awole K, Richards JH, Sen S, Verslues PE, Juenger TE, McKay JK (2015) Exploiting differential gene expression and epistasis to discover candidate genes for drought-associated QTLs in *Arabidopsis thaliana*. Plant Cell **27:** 969–983

Mattioli R, Biancucci M, Lonoce C, Costantino P, Trovato M (2012) Proline is required for male gametophyte development in Arabidopsis. BMC Plant Biol **12:** 236

Meyer Y, Belin C, Delorme-Hinoux V, Reichheld JP, Riondet C (2012) Thioredoxin and glutaredoxin systems in plants: molecular mechanisms, crosstalks, and functional significance. Antioxid Redox Signal **17:** 1124–1160

Miller G, Stein H, Honig A, Kapulnik Y, Zilberstein A (2005) Responsive modes of *Medicago sativa* proline dehydrogenase genes during salt stress and recovery dictate free proline accumulation. Planta **222:** 70–79

Nakashima K, Satoh R, Kiyosue T, Yamaguchi-Shinozaki K, Shinozaki K (1998) A gene encoding proline dehydrogenase is not only induced by proline and hypoosmolarity, but is also developmentally regulated in the reproductive organs of Arabidopsis. Plant Physiol **118:** 1233–1241

Nanjo T, Kobayashi M, Yoshiba Y, Kakubari Y, Yamaguchi-Shinozaki K, Shinozaki K (1999) Antisense suppression of proline degradation improves tolerance to freezing and salinity in Arabidopsis thaliana. FEBS Lett **461:** 205–210

Nobusawa T, Okushima Y, Nagata N, Kojima M, Sakakibara H, Umeda M (2013) Synthesis of very-long-chain fatty acids in the epidermis controls plant organ growth by restricting cell proliferation. PLoS Biol **11:** e1001531

Oshima Y, Shikata M, Koyama T, Ohtsubo N, Mitsuda N, Ohme-Takagi M (2013) MIXTA-like transcription factors and WAX INDUCER1/SHINE1 coordinately regulate cuticle development in *Arabidopsis* and *Torenia fournieri*. Plant Cell **25:** 1609–1624

Pastore D, Trono D, Laus MN, Di Fonzo N, Flagella Z (2007) Possible plant mitochondria involvement in cell adaptation to drought stress. A case study: durum wheat mitochondria. J Exp Bot **58:** 195–210

Peng Z, Lu Q, Verma DPS (1996) Reciprocal regulation of delta 1-pyrroline-5-carboxylate synthetase and proline dehydrogenase genes controls proline levels during and after osmotic stress in plants. Mol Gen Genet **253:** 334–341

Rasmusson AG, Wallström SV (2010) Involvement of mitochondria in the control of plant cell NAD(P)H reduction levels. Biochem Soc Trans **38:** 661–666

Roosens NH, Al Bitar F, Loenders K, Angenon G, Jacobs M (2002) Overexpression of ornithine-delta-aminotransferase increases proline biosynthesis and confers osmotolerance in transgenic plants. Mol Breed **9:** 73–80

Satoh R, Fujita Y, Nakashima K, Shinozaki K, Yamaguchi-Shinozaki K (2004) A novel subgroup of bZIP proteins functions as transcriptional activators in hypoosmolarity-responsive expression of the ProDH gene in Arabidopsis. Plant Cell Physiol **45:** 309–317

Satoh R, Nakashima K, Seki M, Shinozaki K, Yamaguchi-Shinozaki K (2002) ACTCAT, a novel cis-acting element for proline- and hypoosmolarity-responsive expression of the ProDH gene encoding proline dehydrogenase in Arabidopsis. Plant Physiol **130:** 709–719

Sawahel WA, Hassan AH (2002) Generation of transgenic wheat plants producing high levels of the osmoprotectant proline. Biotechnol Lett **24:** 721–725

Schertl P, Cabassa C, Saadallah K, Bordenave M, Savouré A, Braun HP (2014) Biochemical characterization of proline dehydrogenase in Arabidopsis mitochondria. FEBS J **281:** 2794–2804

Schnurr J, Shockey J, Browse J (2004) The acyl-CoA synthetase encoded by LACS2 is essential for normal cuticle development in *Arabidopsis*. Plant Cell **16:** 629–642

Senthil-Kumar M, Mysore KS (2012) Ornithine-delta-aminotransferase and proline dehydrogenase genes play a role in non-host disease resistance by regulating pyrroline-5-carboxylate metabolism-induced hypersensitive response. Plant Cell Environ **35:** 1329–1343

Servet C, Ghelis T, Richard L, Zilberstein A, Savoure A (2012) Proline dehydrogenase: a key enzyme in controlling cellular homeostasis. Front Biosci (Landmark Ed) **17:** 607–620

Sharma S, Verslues PE (2010) Mechanisms independent of abscisic acid (ABA) or proline feedback have a predominant role in transcriptional regulation of proline metabolism during low water potential and stress recovery. Plant Cell Environ **33:** 1838–1851

Sharma S, Villamor JG, Verslues PE (2011) Essential role of tissue-specific proline synthesis and catabolism in growth and redox balance at low water potential. Plant Physiol **157:** 292–304

Skirycz A, De Bodt S, Obata T, De Clercq I, Claeys H, De Rycke R, Andriankaja M, Van Aken O, Van Breusegem F, Fernie AR, et al (2010) Developmental stage specificity and the role of mitochondrial metabolism in the response of Arabidopsis leaves to prolonged mild osmotic stress. Plant Physiol **152:** 226–244

Su J, Wu R (2004) Stress-inducible synthesis of proline in transgenic rice confers faster growth under stress conditions than that with constitutive synthesis. Plant Sci **166:** 941–948

Szabados L, Savouré A (2010) Proline: a multifunctional amino acid. Trends Plant Sci **15:** 89–97

Székely G, Abrahám E, Cséplo A, Rigó G, Zsigmond L, Csiszár J, Ayaydin F, Strizhov N, Jásik J, Schmelzer E, et al (2008) Duplicated P5CS genes of Arabidopsis play distinct roles in stress regulation and developmental control of proline biosynthesis. Plant J **53:** 11–28

Trenkamp S, Martin W, Tietjen K (2004) Specific and differential inhibition of very-long-chain fatty acid elongases from Arabidopsis thaliana by different herbicides. Proc Natl Acad Sci USA **101:** 11903–11908

Verslues PE (2010) Quantification of water stress-induced osmotic adjustment and proline accumulation for *Arabidopsis thaliana* molecular genetic studies. *In* R Sunkar, ed, Plant Stress Tolerance: Methods and Protocols. Humana Press, New York, pp 301–316

Verslues PE, Sharma S (2010) Proline metabolism and its implications for plant-environment interaction. The Arabidopsis Book **8:** e0140 doi/10.1199/tab.0140

Voetberg GS, Sharp RE (1991) Growth of the maize primary root at low water potentials. III. Role of increased proline deposition in osmotic adjustment. Plant Physiol **96:** 1125–1130

Wang Y, Wu JF, Nakamichi N, Sakakibara H, Nam HG, Wu SH (2011a) LIGHT-REGULATED WD1 and PSEUDO-RESPONSE REGULATOR9 form a positive feedback regulatory loop in the *Arabidopsis* circadian clock. Plant Cell **23:** 486–498

Wang ZY, Xiong L, Li W, Zhu JK, Zhu J (2011b) The plant cuticle is required for osmotic stress regulation of abscisic acid biosynthesis and osmotic stress tolerance in *Arabidopsis*. Plant Cell **23:** 1971–1984

Weigel D, Glazebrook J (2002) Arabidopsis: A laboratory manual. Cold Spring Harbor Laboratory Press, NY

Weltmeier F, Ehlert A, Mayer CS, Dietrich K, Wang X, Schütze K, Alonso R, Harter K, Vicente-Carbajosa J, Dröge-Laser W (2006) Combinatorial control of Arabidopsis proline dehydrogenase transcription by specific heterodimerisation of bZIP transcription factors. EMBO J **25:** 3133–3143

Xiao F, Goodwin SM, Xiao Y, Sun Z, Baker D, Tang X, Jenks MA, Zhou JM (2004) Arabidopsis CYP86A2 represses Pseudomonas syringae type III genes and is required for cuticle development. EMBO J **23:** 2903–2913

Yoshiba Y, Kiyosue T, Nakashima K, Yamaguchi-Shinozaki K, Shinozaki K (1997) Regulation of levels of proline as an osmolyte in plants under water stress. Plant Cell Physiol **38:** 1095–1102

Zhang CS, Lu Q, Verma DPS (1995) Removal of feedback inhibition of delta 1-pyrroline-5-carboxylate synthetase, a bifunctional enzyme catalyzing the first two steps of proline biosynthesis in plants. J Biol Chem **270:** 20491–20496

Zhang L, Becker DF (2015) Connecting proline metabolism and signaling pathways in plant senescence. Front Plant Sci **6:** 552

Zhu BC, Su J, Chan MC, Verma DPS, Fan YL, Wu R (1998) Overexpression of a Δ^1-pyrroline-5-carboxylate synthetase gene and analysis of tolerance to water- and salt-stress in transgenic rice. Plant Sci **139:** 41–48

Zsigmond L, Rigó G, Szarka A, Székely G, Otvös K, Darula Z, Medzihradszky KF, Koncz C, Koncz Z, Szabados L (2008) Arabidopsis PPR40 connects abiotic stress responses to mitochondrial electron transport. Plant Physiol **146:** 1721–1737